OBSERVATIONAL EVIDENCES FOR HEATING OF THE SOLAR CORONA BY NANOFLARES IN THE NETWORK DERIVED FROM THE TRANSITION REGION SPECTRAL LINES

Ján Rybák[(1)], Aleš Kučera[(1)], Werner Curdt[(2)], and Hubertus Wöhl[(3)]

[(1)]*Astronomical Institute, SAS, 05960 Tatranská Lomnica, Slovakia*
[(2)]*Max-Planck-Institut für Sonnensystemforschung, 37191 Katlenburg-Lindau, Germany*
[(3)]*Kiepenheuer-Institut für Sonnenphysik, 79104 Freiburg, Germany*

ABSTRACT

SUMER/SOHO measurements of the transition region C II 1037.0 Å (3×10^4 K) and O VI 1031.9 Å (2.8×10^5 K) emission lines in a distinctive network of the quiet solar atmosphere are used to search for consequences of the possible nanoflare heating of the corona. A statistical analysis of the central line intensity and the line shift of these lines has revealed for the studied network: 1/ systematically larger values of the line shifts in the network relatively to internetwork; 2/ distinct dependence of the line shifts and on the line intensities (comparing to internetwork reference) in the form of separated 'clusters' of data coming from in the network and internetwork; 3/ no correlation between the line shifts and the line intensities in the network. A case study of the particular O VI spectral profiles has shown that at least some of the significantly broadened O VI line profiles consist in fact of two Gaussian profiles: one referring to a central less shifted component and the other to a weak more redshifted component. These findings are compared to results of other observational studies as well as to results of MHD simulations of the magnetic loops in the outer solar atmosphere in which the nanoflare heating mechanism was incorporated. Our preliminary results show that the derived observational facts are consistent with effects of fast magneto-acoustic modes, predicted to be caused by nanoflares, travelling downward along the loops in network. Nevertheless an agreement can be found only when spatial and temporal smearing of measurements are taken into account.

1. INTRODUCTION

Parker (1988) proposed that coronal heating could be achieved by the sum of the heat deposited by small reconnection events caused by the low-frequency random motion of the footpoints of coronal magnetic flux tubes. Energy of an order of $10^{23} - 10^{25}$ ergs released in a small volume in one nanoflare should excite magneto-hydrodynamic waves in the coronal low β plasma (Parker, 1994). A response of the nanoflare heating mechanism in the transition region plasma was modelled simulating effects of the downward propagating modes of these waves in papers of Hansteen (1993) and Hansteen et al. (1996) attempting to explain the pervasive redshift of the transition region spectral lines. Effects of both the downward and also possible upward propagating waves on properties of the transition region lines were investigated by Wikstøl et al. (1998). It was found that the proposed signatures of waves in the profiles of the transition region lines are only very subtle when the spatial/temporal/spectral resolution of the existing instruments are considered. Therefore a new diagnostic tool was developed and tested in order to confirm the direction of wave propagation using the ratios of spectral line profiles (Wikstøl et al., 1997, Judge et al., 1998). Nevertheless the first statistical evidence for the average redshift of transition region lines as an effect of downward propagating waves generated by nanoflares in the corona was presented by Hansteen et al. (2000). This contribution is aimed to search for new direct observational evidence for downward propagating waves exhibited by the profiles of transition region lines. Comparison to the statistical observational evidence will be also presented and discussed.

2. DATA

The SUMER spectrometer is a high-resolution normal-incidence spectrometer on SOHO mission allowing to investigate solar processes temperature range from 10^4 to 2×10^6 K with high spatial, spectral and temporal resolution in the EUV spectral range (Wilhelm et al., 1995). Summaries of its in-flight performance were presented in papers of Wilhelm et al. (1997) and Lemaire et al. (1997). The SUMER data set, analyzed in this contribution, has been acquired on 5 May 1999 ($8^h25.5^m - 9^h40.5^m$) as a part of the joint observing program JOP 78.[1] The set consists of a time series of 300 spectral images 50 pixels wide covering the spectral range 1035.7 – 1038.7 Å. with two emission lines of C II and one line of O VI. The integration time was 15 s, limited by the telemetry rate. Data were acquired on the KBr part of detector B using the 0.38"×120" entrance slit oriented in the NS direction. Compensation of the solar rotation has been applied as the slit has moved for 0.38" after each 10 exposures. Therefore the slit has rastered each 150 s a very narrow area only 0.76" wide in the EW direction. A quiet sun area ∼250" away from the disk center was selected as target to avoid active regions visible on the disk. For this contribution the slit length was truncated just to 65" covering the internetwork and one particular network area (Fig.1).

[1] JOP 078 proposal: www.astro.sk/∼choc/jop078_prop/

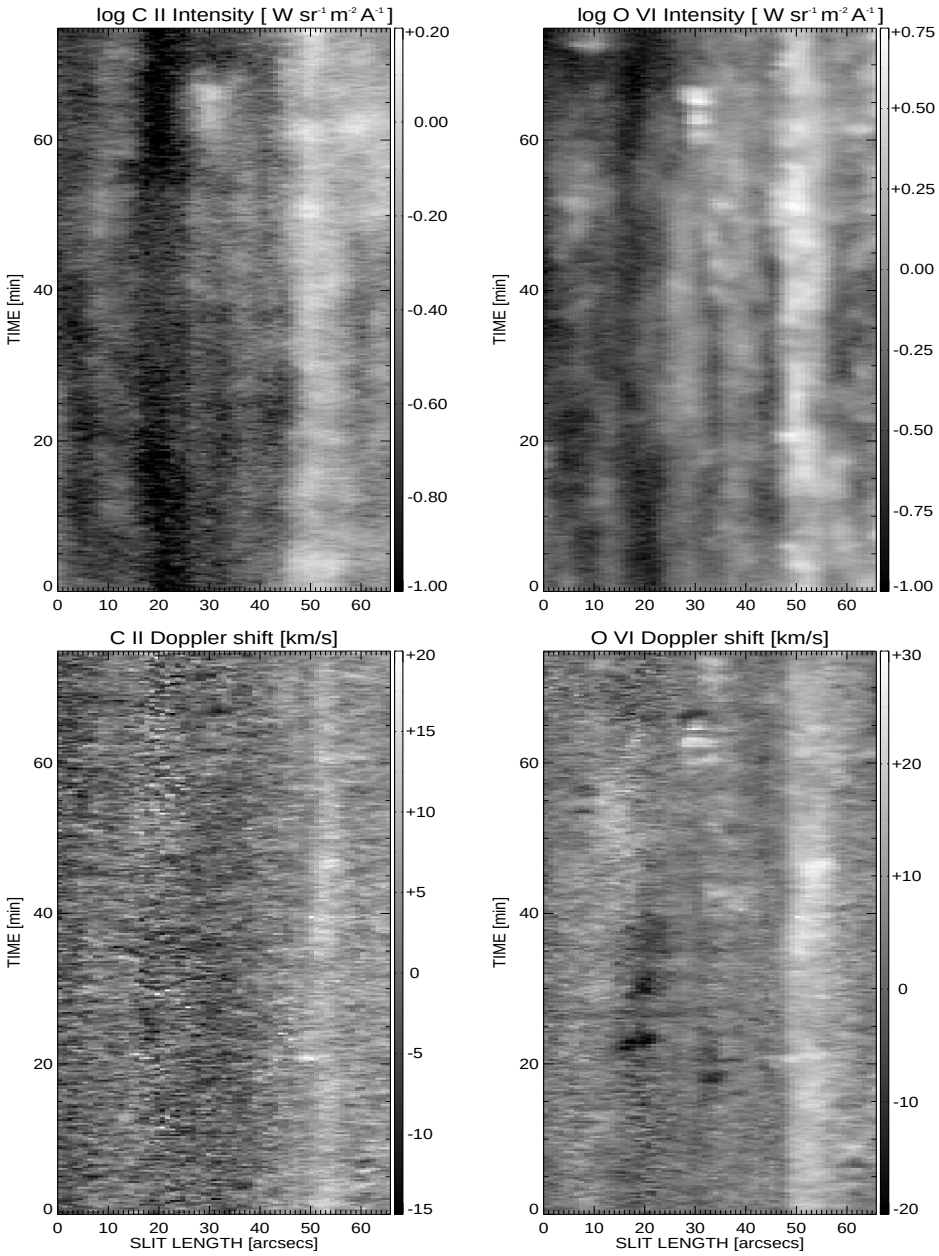

Figure 1. Space-time behaviour of the central line intensities (logarithmic scale, top row panels), the line shifts (bottom row, positive values – redshift) of the C II (left column) and O VI (right column) lines. In particular, the internetwork within the slit range 15" – 25" and the narrow network area in the range just 3" broad centred at 50" were selected for analysis in this contribution.

3. DATA REDUCTION

The basic reduction of data was performed with help of the standard SUMER reduction procedures.[2] The relative sensitivities of the pixels of the detector were taken into account using the deep flat-field data obtained on 18th March 1999. Temporal shifts of the flat-field pattern have been determined and the advanced flat field correction was applied with the odd-even pattern corrected first and then the shifted flat-field pattern was taken into account.[2] Aberrations of the spectral images were corrected using the available destretching algorithm and its auxiliary data. The thermoelastic oscillations of the spectrometer mechanical structure (Curdt et al., 1997) were determined using positions of the C II lines and the residual shift of the spectral image of up to 0.8 pixel was found. Correction was applied with the line shift uncertainty less than 1 km/s using the procedure described by Rybák et al. (1999). Data were also converted to physical units using the radiometry procedure.[3]

[2] Standard SUMER reduction procedures: www.linmpi.mpg.de/english/projekte/sumer/text/cookbook.html

[3] SUMER radiometry procedure: www.linmpi.mpg.de/english/projekte/sumer/text/radcal.html

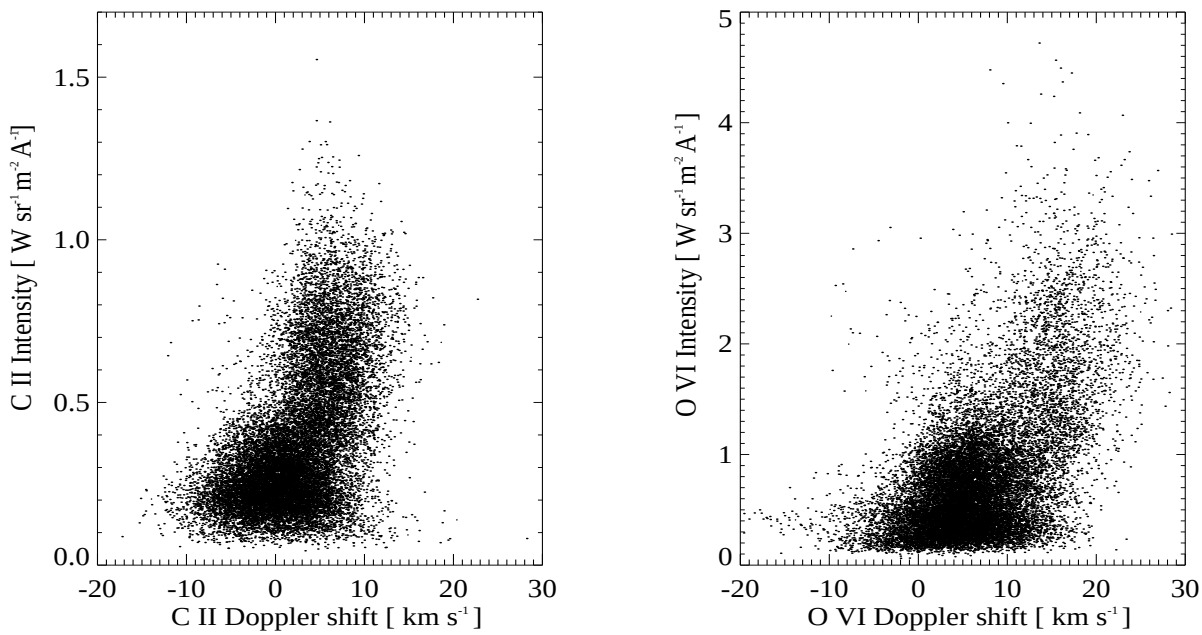

Figure 2. Scatter plots presenting dependences between the line intensity and the line shift for the C II (left panel) and O VI (right panel) lines for the whole time-space domain (65”×75 min) presented in Fig.1.

Our wavelength calibration is based on the assumption that chromospheric lines of neutral atoms (or lines of lower formation temperature) should statistically exhibit no significant line shifts as compared to the large line shifts of the transition region lines. Thus the calibration of the relative wavelength scale was performed using spectra of two C II lines acquired in the internetwork region and the laboratory wavelengths data of Kelly (1987).

Finally each spectral profile containing two C II and one O VI line was fitted using a triple Gauss fit with constant background. The CFIT algorithm[4] of S.V.H. Haugan was used for this exercise using the relative weighting of the data. The data weights were determined according to Poisson noise statistics with noise estimated by the square root of the counts (instrumental units). The CFIT algorithm determines the best fit by minimizing the reduced squared residuals χ_r^2 defined as

$$\chi_r^2 = \frac{1}{N-M}\sum_{i=1}^{N}\frac{(y_i - y(x_i; a_1, ..., a_M))^2}{\sigma_i^2}, \qquad (1)$$

where σ_i is the weight for each spectral point (x_i, y_i), y is the fitted value for x_i, N is number of spectral points, and M is number of the parameters a_j of the fitted function. In this way the central line intensity, the line width and the line shift (Doppler shift) were determined for each line together with the underlying continuum intensity.

4. RESULTS AND DISCUSSION

For a statistical analysis of the central line intensity and the line shifts of the C II and O VI lines scatter plots of inter-relations were prepared for two examples with different space-time domains.

The first example utilises the domain covering a large spatial area of both network and internetwork including locations of an intermediate activity (in the line intensity) between the line internsities and the line shifts (whole domain shown in Fig.1). The scatter plots of inter-relations between the spectral parameters (Fig.2) show that:

- systematically larger values of the line shifts in the network relatively to internetwork seems to confirm existence of a correlation of the line redshift with the line intensity (for both C II and O VI lines). Our results are in agreement with the recent observational results of Hansteen et al. (2000) but in contradiction to the findings of Dere et al. (1984)
- the scatter plots seem to consist of two separated ’clusters’ of data: one ’cluster’ for internetwork and another for network

The possible existence of two separated ’clusters’ of data has motivated us to prepare the second example for which the truncated space-time domain of 10”×75 min and 3”×75 min was selected for the internetwork and network, respectively. The internetwork domain covers just the very quiet area where the lowest values of the line intensities were acquired. The network domain was selected as a very narrow region where strong emissions in both investigated lines lasted during the whole selected time and over the slit length 3” (Fig. 1). The scatter plots of relations between the spectral parameters prepared for the second example (Fig.3) reveal the following for the selected distinctive network:

[4]CFIT description: solg2.bnsc.rl.ac.uk/swnotes/

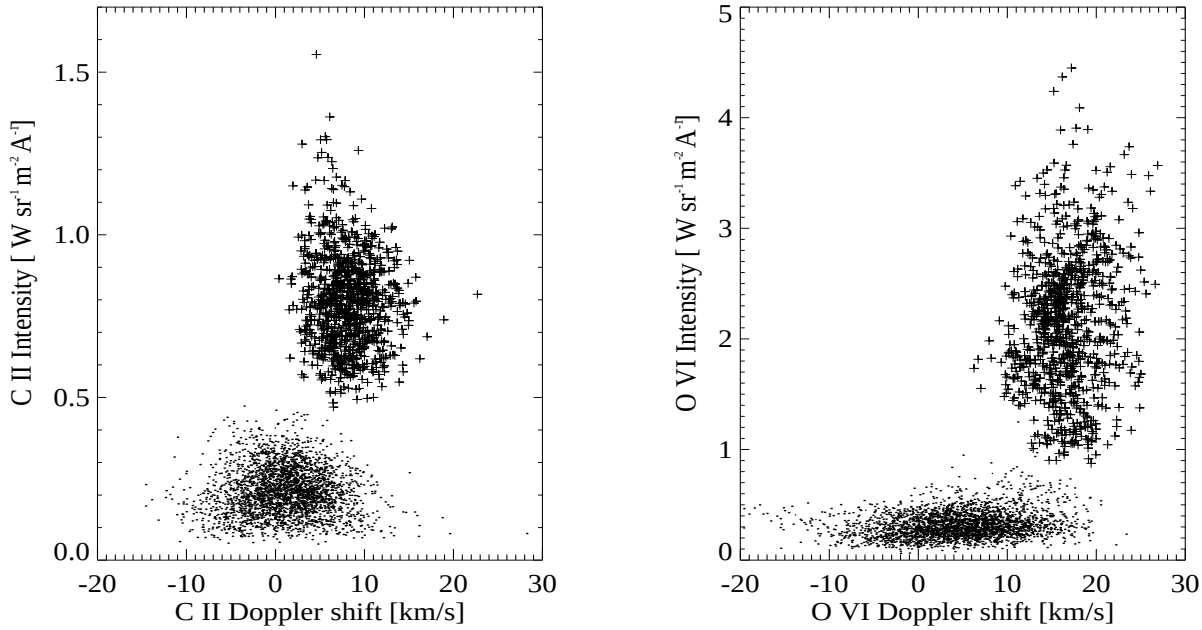

Figure 3. Scatter plots showing a relation between the line intensity and the line shift for both the C II line (left panel) and the O VI line (right panel) for the particular time-space domains of the internetwork (dots) and the narrow network region (plus signs) in an identical layout as in Fig.2 for the whole time-space domain. Altogether 3000 internetwork and 900 network data points covering the domains of 10”×75 min and 3”×75 min were used, respectively.

- data indeed show clear separation of the internetwork and network for all relations
- significant redshift in the network relatively to internetwork is detected, the average of the redshift data is ∼8km/s and ∼12km/s for the C II and O VI lines respectively
- nevertheless no correlation of the line intensity with the line redshift is seen for this distinctive network although significant variations of the line intensity were derived

These results seem to be in contradiction with the previously obtained observational results of Hansteen et al. (2000) as well as with predictions of the MHD numerical simulations of the magnetic loops in the outer solar atmosphere in which the nanoflare heating mechanism was incorporated (Hansteen, 1993). Both studies show correlation of the line redshift with the line intensity. Nevertheless, in our opinion, difference in the observational results can be explained by the fact that when identifying the network in similar studies usually an rectangular space–time domain is selected which covers also areas of the intermediate intensity of the transition region lines (e.g., Wikstøl et al., 2000, Hansteen et al., 2000, our Fig.1). In particular, these areas of the intermediate values of the line intensity and redshift are filling the gap between the ’clusters’ producing finally a continuous transition from low values of line intensity and line shift to higher ones. This conclusion is also supported by the results which were obtained using our data when range of the slit length for the network separation was prolonged from 3” to larger fractions of the total slit length (not shown here).

On the other hand, the apparent contradiction between our results and the results of numerical simulations concerning the correlation can be solved. Predictions of the numerical simulations (Hansteen, 1993, Hansteen et al., 1996, Wikstøl et al., 1997) indeed display that the highest intensities of lines appear only for the significantly redshifted profiles of the transition region line over a broad range of temperatures. However, the duration of the MHD wave passage is very short and these pulses of the enhanced and redshifted emission should be shorter than just 1 s (Wikstøl et al., 1997, Hansteen et al., 2000). While the long exposure time of the used spectra (15 s) and the accumulation of the emission from the optically thin line along the line-of-sight as well as the limited spatial resolution (theoretically ∼1”×0.4”) are taken into account a filling factor of the order of 10^{-3} can be assumed. Using the predicted values of the parameters of such a pulse derived from numerical simulations (Hansteen, 1993, Hansteen et al., 1996, Wikstøl et al., 1997) it can be estimated that the intensity of a typical transition region line of the redshifted line component could be of the order of 10^{-1} and the redshift of this line component can be up the order of 10^2 km/s.

We have performed a search for examples of line profiles of the C II and O VI lines in order to find possible evidence of these predictions in our data set. Here we document only the best example as a ’Case I’ located in the network (slit position = 48”, time = 20.8 min in the panels of Fig.1). The line profiles of the C II and the O VI line were fitted using one Gaussian profile per line as well as using two Gaussian profiles for the O VI line as the particular profile of this line has revealed a clear two-component structure (Fig.4). The multiple nature of the

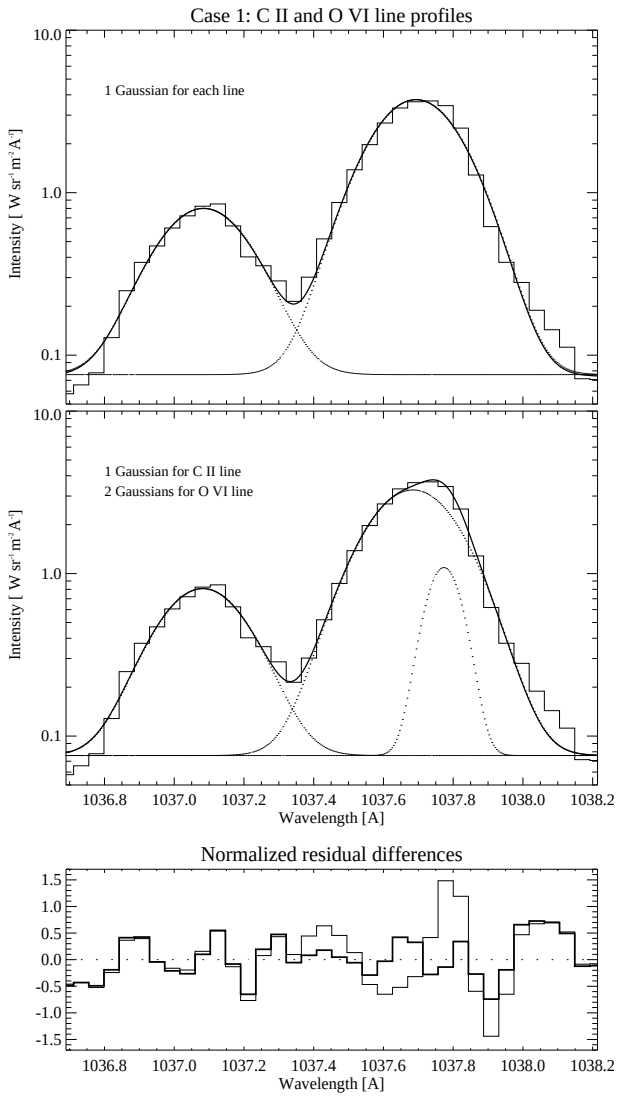

Figure 4. Fits of the spectral profiles of the C II *and O* VI *lines for case I. The top panel shows the fitting results using one Gaussian for each line and the middle panel results when two Gaussians are used for the O* VI *line (histogram – the measured spectrum, dotted lines – individual Gaussian profiles of C* II *and O* VI *lines, full solid line – result of the fitted spectrum as the sum of the individual Gaussian profiles and the underlying continuum intensity). The bottom panel displays the normalized residual differences between the measured and fitted spectrum when one Gaussian for each line was used (thin line) and when two Gaussians are used for the O* VI *line (thick line).*

O VI line is visualized also by the decrease of the normalized residual differences between the observed and fitted spectrum. Maximum intensity of the weak, more redshifted, component of the O VI line is about ∼1/3 of the central intensity of the strong core component and it is redshifted by ∼45 km/s from its laboratory wavelength while the strong core component is redshifted just by ∼20 km/s. The total emission of the weak component is 12 % of the total emission of the strong, less redshifted, component. Although the weak component seems to be very faint, once we speculate about pulses of the enhanced and redshifted emission being shorter than 1 s (Wikstøl et al., 1997, Hansteen et al., 2000), we can conclude that this more redshifted component could in pulses be dominant in both the central intensity and total emission even the line width of this component is just ∼40 % of the strong one. The presented example of 'Case I' might help us to understand the pervasive redshift observed in the transition region spectral lines. It shows how the typical, presently used, exposure times of UV spectral lines (∼10 s) can average in time several short-lived emission spikes of different line intensity (and line width) to a smeared, but redshifted, spectral profile. Of course, also alternative mechanisms, which could cause such effects in the transition region line profiles, have to be investigated, e.g., condensation in cool loops (Müller et al., 2003); footpoint dynamics of a coronal loop (McIntosh and Poland, 2004); appearance of active events in the network - blinkers and/or explosive events.

Concerning planned future missions it seems that besides of the generally accepted increasing of the spatial resolution of the proposed UV spectrometers additional improvement of the instrument throughput and/or detector sensitivity should be essential for studies similar to this one. It seems that exploiting the excellent data provided by the SUMER spectrometer (Wilhelm et al., 1995) with its high spatial resolution (Lemaire et al., 1997) we see that for the future strong need to add higher temporal sampling of ∼1 s together with an improvement of the S/N ratio of the UV spectra will be essential for studies similar to the present one.

5. CONCLUSION

The following preliminary conclusions result from the performed statistical analysis of the central line intensity and the line shift of the C II and O VI lines for the selected distinctive network:

- there are systematically larger values of the line shifts in the network relatively to internetwork while in particular distinct dependence of the line shifts on the line intensities were found in the form of the separated 'clusters' of data coming from in the network and internetwork;
- no correlation was found between the line shifts and the line intensities in the network;

Our case study of the particular O VI spectral profiles has shown that at least some of the significantly broadened O VI line profiles are in fact consisting of two Gaussian profiles: one referring to a central, less shifted, component and the other to a weak, more redshifted, component. This observational fact could help to understand the pervasive redshift observed in transition region spectral lines. It was shown that typical exposure times of

UV spectral lines of $\sim$10 s can average in time short-lived emission excursions both in line intensity and line shift producing a smeared but redshifted spectral profile. Our preliminary observational findings do not contradict the predictions of MHD numerical simulations of magnetic loops in the outer solar atmosphere in which the nanoflare heating mechanism was incorporated. Nevertheless a qualitative agreement can be found only when spatial and temporal smearing introduced by measurements are taken into account.

ACKNOWLEDGMENTS

SOHO is a project of international cooperation between ESA and NASA. The SUMER project is financially supported by DLR, CNES, NASA, ESA and PRODEX (Swiss contribution). Additional support was provided by the participating institutions. A.K. and J.R. are grateful to the Slovak grant agency VEGA for supporting of this work (grant No. 2/3015/23). This research is part of the European Solar Magnetism Network (EC/RTN contract HPRN-CT-2002-00313).

REFERENCES

Curdt, W., Kučera, A., Rybák, J., Schühle, U., Wöhl, H.: 1997, in *Fifth SOHO Workshop 'The Corona and the Solar Wind near Minimum Activity'*, ed. A.Wilson, ESA SP-404, ESA, Noordwiijk, Netherlands, 307

Dere, K, P., Bartoe, J.-D. F., Brueckner, G. E.: 1984, *Astrophys. J.* **281**, 870

Hansteen, V.: 1993, *Astrophys. J.* **402**, 741

Hansteen, V., Maltby, P., Malagoli, A.: 1996, in *'Magnetic Reconnection in the Solar Atmosphere'*, eds. R.D. Bentley and J.T. Mariska, ASP Conference Series **111**, 116

Hansteen, V., Betta, R., Carlsson, M.: 2000, *Astron. Astrophys.* **360**, 742

Judge, P. G., Hansteen, V., Wikstøl, Ø., Wilhelm, K., Schühle, U., Moran, T.: 1998, *Astrophys. J.* **502**, 981

Kelly, R. L: 1987, *J. Phys. Chem. Ref. Data* **16**, 1

Lemaire, P., Wilhelm, K., Curdt, W. et al.: 1997, *Solar Phys.* **170**, 105

McIntosh, S. W, Poland, A. I.: 2004, *Astrophys. J.* **604**, 449

Müller, D. A. N., Hansteen, V. H., Peter, H.: 2003, *Astron. Astrophys.* **411**, 605

Parker, E. N.: 1988, *Astrophys. J.* **330**, 474

Parker, E. N.: 1994, *Spontaneous Current Sheets in Magnetic Fields*, Oxford University Press, New York

Rybák, J., Curdt, W., Kučera, A., Schühle, U., Wöhl, H.: 1999, in : *Proceedings of the 9th European Meeting on Solar Physics 'Magnetic fields and Solar Processes'*, ed. A. Wilson, ESA SP-448, Noordwiijk, Netherlands, 361

Wikstøl, Ø., Judge, P. G., Hansteen, V. H.: 1997, *Astrophys. J.* **483**, 972

Wikstøl, Ø., Judge, P. G., Hansteen, V.: 1998, *Astrophys. J.* **501**, 895

Wikstøl, Ø., Hansteen, V. H., Carlsson, M.: 2000, *Astron. Astrophys.* **531**, 1150

Wilhelm, K., Curdt, W., Marsch, E., Schühle, U., Lemaire, P., Gabriel, A., Vial, J.-C., Grewing, M., Huber, M. C. E., Jordan, S. D., Poland, A. I., Thomas, R. J., Kühne, M., Timothy, J. G., Hassler, D. M., and Siegmund, O. H. W.: 1995, *Solar Phys.* **162**, 189

Wilhelm, K. et al., 1997, *Solar Phys.* **170**, 75